Multi-Terminal VSC-HVDC System for Integration of Offshore Wind Farms and Green Electrification of Platforms in the North Sea

Temesgen M. Haileselassie, Marta Molinas, *Member, IEEE*, Tore Undeland, *Fellow, IEEE*,

***Abstract*—This paper discusses a multi-terminal VSC-HVDC system proposed for integration of deep sea wind farms and offshore oil and gas platforms in to the Norwegian national grid onshore. An equivalent circuit of the VSC in synchronous d-q reference frame has been established and decoupled control of active and reactive power was developed. A three terminal VSC-HVDC was modeled and simulated in EMTDC/PSCAD software. Voltage margin method has been used for reliable operation of the HVDC system without the need of communication. Simulation results show that the proposed multi-terminal VSC-HVDC was able to maintain constant DC voltage operation during load switchings, step changes in power demand and was able to secure power to passive loads during loss of a DC voltage regulating VSC-HVDC terminal with out the use of communication between terminals.**

***Index Terms*—Multi-terminal HVDC, EMTDC/PSCAD, Voltage Source Converters, vector control**

I. Introduction

INTENSIVE research efforts are underway in Norway towards developing large scale deep sea wind farms with expected distances of 100-300 Km from shore [1]. For reasons of large capacitive currents HVAC will not be a technically and economically feasible solution for such submarine distances [7],[9]. This makes HVDC the more feasible solution in this particular case.

On the other hand, the Norwegian oil and gas platforms, which currently use gas turbines except in one case (Troll A [2]), contribute towards a large share of the total CO_2 emission in Norway [10]. For economic and environmental protection reasons there has been a tendency towards replacing the gas turbines with electric supply from onshore grid [8].

An interconnection between the offshore wind farms, the oil and gas platforms and onshore grid can result in reduced operational costs, increased reliability and reduced CO_2 emissions. A multi-terminal HVDC (MTDC) network will then be the core of such an interconnection system. MTDC can also open new power market opportunities and result in better utilization of transmission lines [11].

Temesgen M. Haileselassie, M. Molinas and T. Undeland are with the Department of Electric Power Engineering, Norwegian University of Science and Technology, Trondheim N-7491, Norway (e-mail: hailesel@stud.ntnu.no, marta.molinas@elkraft.ntnu.no, Tore.Undeland@elkraft.ntnu.no)
Fax: +47 7359 4279

Classical HVDC based upon line commutated converters has a main challenge in that it needs reversal of voltage polarity during reversal of power flow. This means that classical HVDC is unable to operate at fixed DC voltage level for both rectifier mode and inverter mode of operation. Since maintaining a constant dc voltage during all conditions is one expected and important feature of the MTDC, the thyristor based classical HVDC may not be a good candidate in developing MTDC.

Voltage source converters (VSC) on the other hand do not need reversal of polarity for changing the direction of power flow and also are capable of independent control of active and reactive power. This makes VSC and ideal component in making MTDC.

This paper presents a proposed three terminal VSC-HVDC model linking an onshore grid, offshore wind farm and offshore oil and gas platform and discusses the control strategy for the terminals.

II. Equivalent Circuit of Vsc in Synchronous d-q Reference Frame

A. Voltage Source Converter

A schematic view of voltage source converter is shown in Figure 1. The series inductance on the ac side, also called ac reactor, smoothens the sinusoidal current on the ac network and is also useful for providing the reference point for ac voltage, current and active and reactive power measurements. The shunt connected capacitors on the DC network side are used for DC voltage source and harmonic attenuation.

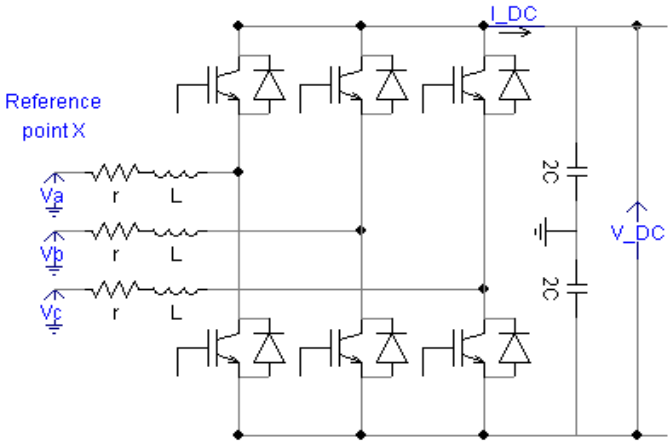

Figure 1. Schematic of VSC

Usually, a VSC station works in either of the four control modes listed below [3].

a. Constant active power control
b. Constant DC voltage control
c. Constant DC current control
d. Constant AC voltage control

In this paper active power control, DC voltage control and AC voltage control will be used at different terminals to establish an MTDC network.

B. Single line diagram representation

A single line diagram of a VSC is shown below in figure 2.

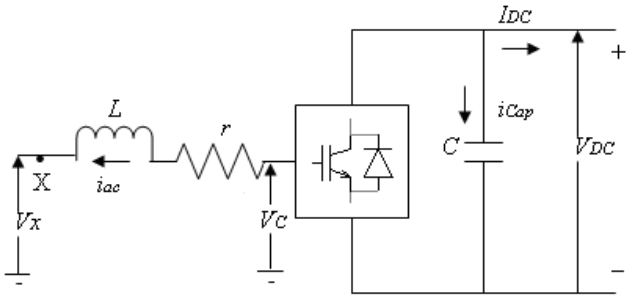

Figure 2. Single line diagram representation of VSC

The reference point for measuring active power, reactive power, and voltage is point X in Figure 2.

Voltage across the ac reactor in abc reference frame is given by:

$$V_{Cabc} - V_{xabc} = L\frac{di_{abc}}{dt} + ri_{abc} \tag{2}$$

C. Synchronous d-q reference frame

In order to decouple the active and reactive power controls, the synchronously rotating d-q reference frame will be used for developing the controllers. All the phase quantities will first be transformed in to the α-β reference using the Clark transformation (equation 3) [4][12].

$$\begin{pmatrix} \alpha \\ \beta \\ o \end{pmatrix} = \frac{2}{3}\begin{pmatrix} 1 & -\frac{1}{2} & -\frac{1}{2} \\ 0 & \frac{\sqrt{3}}{2} & -\frac{\sqrt{3}}{2} \\ \frac{1}{2} & \frac{1}{2} & \frac{1}{2} \end{pmatrix}\begin{pmatrix} a \\ b \\ c \end{pmatrix} \tag{3}$$

Transforming equation (2) in to α-β representation:

$$V_{C\alpha\beta} - V_{x\alpha\beta} = L\frac{di_{\alpha\beta}}{dt} + ri_{\alpha\beta} \tag{4}$$

The relation between α-β and d-q reference frames is given by Park's transformation (equation 5)[12].

$$x_{dq} = x_{\alpha\beta}e^{-j\omega t}\ \ x_{dq} = x_{\alpha\beta}e^{-j\omega t} \tag{5}$$

Where ω is the angular speed of the rotating d-q reference frame and is equal to the radial frequency of the fundamental ac voltage component.

From equations (2) and (5):

$$\begin{aligned} V_{c\alpha\beta} &= V_{cdq}e^{j\omega t} \\ V_{x\alpha\beta} &= V_{xdq}e^{j\omega t} \\ i_{\alpha\beta} &= i_{dq}e^{j\omega t} \end{aligned} \tag{6}$$

From (4) and (6),

$$\begin{aligned} V_{cdq}e^{j\omega t} - V_{xdq}e^{j\omega t} &= L\frac{d\left(i_{dq}e^{j\omega t}\right)}{dt} + ri_{dq}e^{j\omega t} \\ &= e^{j\omega t}L\frac{di_{dq}}{dt} + Li_{dq}\frac{d(e^{j\omega t})}{dt} + ri_{dq}e^{j\omega t} \\ &= e^{j\omega t}L\frac{di_{dq}}{dt} + j\omega Li_{dq}e^{j\omega t} + ri_{dq}e^{j\omega t} \end{aligned} \tag{7}$$

Eliminating $e^{j\omega t}$ from all terms:

$$V_{cdq} - V_{xdq} = L\frac{di_{dq}}{dt} + j\omega Li_{dq} + ri_{dq} \tag{8}$$

Equation 8 defines the mathematical model of the VSC in synchronous d-q reference frame.

The controllers will be developed with reference to d-q quantities and finally the output will be transformed back to the abc stationary frame before it is sent to Pulse Width Modulator (PWM) of the converter.

D. Phase Lock Loop

The Phase Locked Loop (PLL) synchronizes a local oscillator with a reference sinusoidal input. This ensures that the local oscillator is at the same frequency and in phase with the reference input [6]. The local oscillator is voltage controlled oscillator (VCO). The block diagram of a PLL is shown in Figure 3.

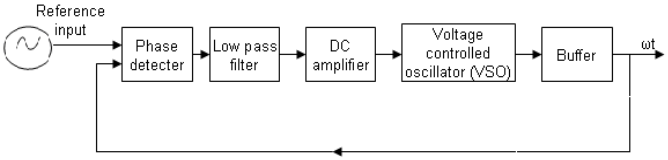

Figure 3. Block diagram of phase lock loop (PLL)

In the VSC the PLL is phase locked with voltage phasor of the phase-a of the reference point. The output of the PLL is

used to synchronize and phase lock the the d-q reference plane with the AC source voltage.

E. Equivalent Circuit in d-q reference frame

The Phase Lock Loop (PLL) that provides with the angle for ab→dq/dq→abc transformation blocks is phase locked with phase a voltage of point X. Moreover, the synchronous d-q reference frame is chosen in order to align the d axis with that of the voltage phasor of phase-a at reference point X in stationary abc reference frame. This results in $V_{Xq}=0$ and $V_{Xd}=V_X$. Then, from equation (8) we get the following simplified relation.

$$\begin{pmatrix} sL+r & 0 \\ 0 & sL+r \end{pmatrix}\begin{pmatrix} i_d \\ i_q \end{pmatrix}=\begin{pmatrix} V_{Cd} \\ V_{Cq} \end{pmatrix}-\begin{pmatrix} V_{Xd} \\ 0 \end{pmatrix}+\begin{pmatrix} 0 & \omega L \\ -\omega L & 0 \end{pmatrix}\begin{pmatrix} i_d \\ i_q \end{pmatrix} \quad (9)$$

From equation (9) the equivalent circuit of the VSC in the synchronized d-q reference frame will be as shown in Figure 4 below.

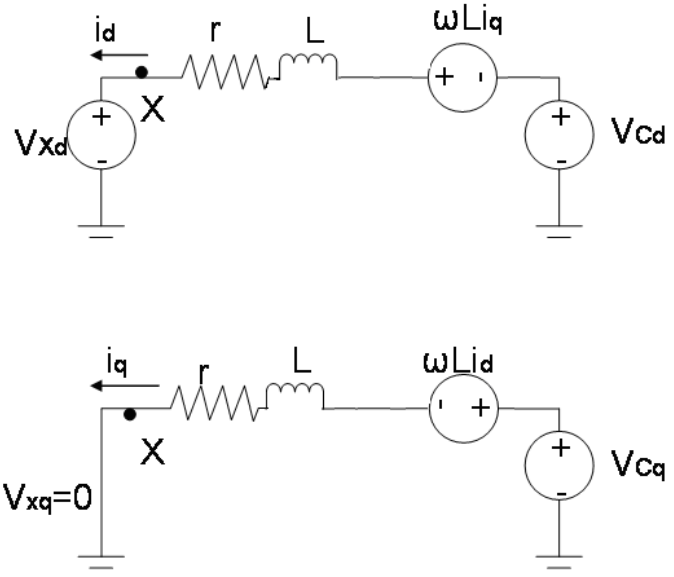

Figure 4. Equivalent circuit diagram of VSC in synchronous d-q reference frame

III. VSC-HVDC CONTROLLERS

A. Inner Current Controllers

The inner current controller can be developed based upon the equivalent circuit in Figure 3 and equation (9) that describes the circuit. Figure 5 shows the d-axis and q-axis current controllers of the inner current loop.

The converter has a delay of $e^{-T_w s} \approx 1/(1+T_w s)$ due to the sinusoidal pulse width modulator and $T_w = 1/2f_s$ where f_s is the switching frequency of the converter. Proportional integral (PI) controllers are used for closed loop control and the zeroes of the PI controllers are selected to cancel the dominant pole in the external circuit. For a typical VSC, the time constant $\tau=L/r$ is much higher than T_w and hence will be the dominant pole to be canceled.

The cross coupling currents in equation (9) are compensated by feed forward terms in the controllers as in Figure 5.

i_d^* and i_q^* are reference currents for the d-axis and q-axis current controllers respectively.

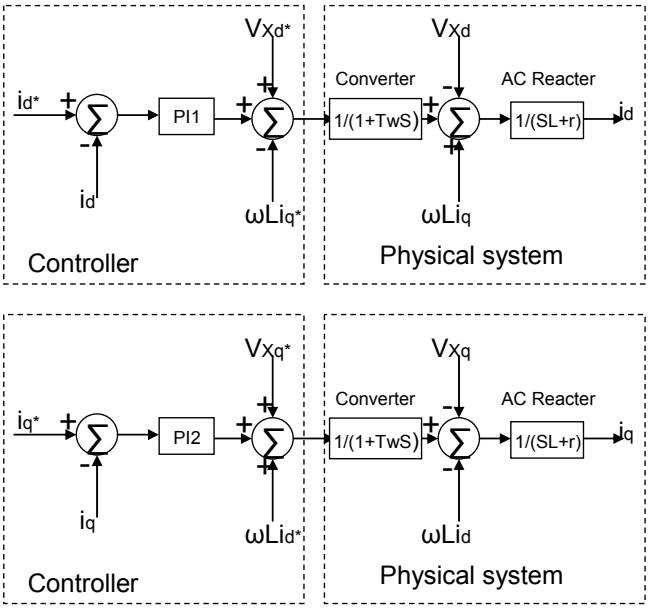

Figure 5: Inner current controllers

B. Outer Controllers

From the d-q equivalent circuit and observing from reference point X, the apparent power injected by the VSC in to the AC network is given by:

$$S=\frac{1}{2}\left(V_{Xd}+j0\right)\left(i_d-ji_q\right) \quad (10)$$

And hence active and reactive powers are given by:

$$P=\frac{3}{2}V_{Xd}i_d \quad (11)$$

$$Q=\frac{-3}{2}V_{Xd}i_q \quad (12)$$

And a small change in the DC voltage can be approximated as:

$$\Delta V_{DC}=\frac{\Delta q_{cap}}{C}=\frac{1}{C}\int i_{cap}dt \quad (13)$$

Where C is the shunt capacitance of the VSC-HVDC, q_{cap} is the charge of the capacitor and i_{cap} is the current going in to the DC capacitor bank as shown in Figure 2. The direction of the currents in the power calculations strictly refer to Figure 2.

From conservation of energy law,

$$\frac{3}{2}V_{Xd}i_d + V_{DC}i_{cap} + V_{DC}I_{DC} = 0 \tag{14}$$

From equations (13) and (14),

$$\frac{d\Delta V_{DC}}{dt} = \frac{-3V_{Xd}}{2CV_{DC}}\left(i_d + \frac{2V_{DC}I_{DC}}{3V_{Xd}}\right) \tag{15}$$

For the sake of simplicity, it is assumed that the VSC-HVDC is connected to a stiff AC network implying that V_{Xd} is also a constant quantity. With such consideration, it can be seen from equations (11), (12) and (15) that active power and DC voltage are correlated with i_d and reactive power with i_q. Hence controller structures will look like as shown in Figure 6.

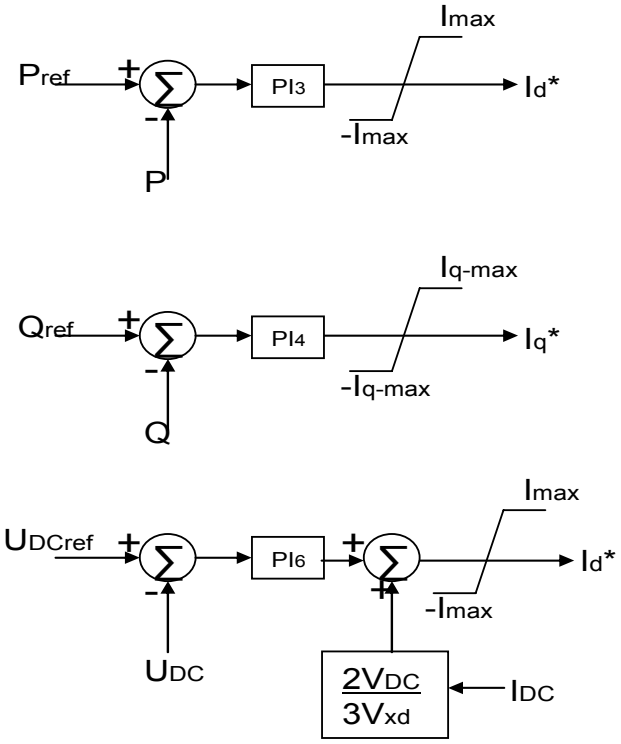

Figure 6. Outer controllers

The DC current is feed forward compensated in the DC voltage controller (Figure 6).

In VSC-HVDC, the maximum current limit of the VSC must not be exceeded at any moment of the operation. On the other hand, priority is given to transfer active power than reactive power. Hence i_d is limited to the maximum current capacity +/-I_{max} and i_q is limited in such a way that the total current will not exceed the rating of the valves. Mathematically:

$$I_{\max} = I_{rated} \tag{16}$$

$$I_{q\max} = \sqrt{\left(I_{rated}^2 - I_d^2\right)} \tag{17}$$

C. VSC-HVDC for Passive Loads

A VSC-HVDC supplying a passive network has the objective of maintaining constant AC voltage for all operating conditions. Active and passive power consumptions depend on the passive network elements and hence are not directly controlled. The fundamental frequency AC voltage output of the converter is given by [13]:

$$V_C = \frac{1}{2}mV_{DC}\sin(\omega t) \tag{18}$$

where m is modulation index of the PWM.

Voltage at the reference point X will be:

$$V_X = \frac{Z_{LD}V_C}{\left(Z_{LD} + j\omega L + r\right)} \tag{19}$$

Where Z_{LD} is the Thevenin equivalent impedance of the ac network at the point of common coupling and is a variable quantity.

From equations (16) and (17), it is seen that the ac voltage can be controlled by controlling the modulation index m as shown in the figure below.

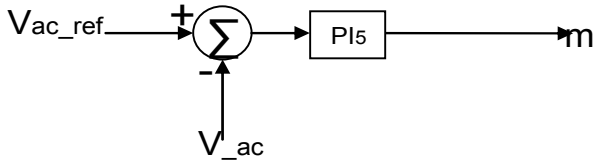

Figure 7. AC voltage regulation by control of modulation index

The complete assembly of the outer and inner controllers is shown in Figure 8 below.

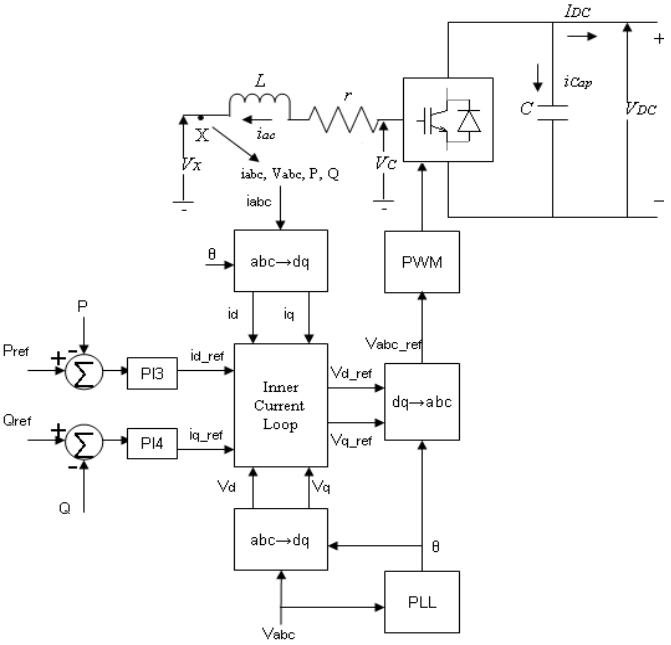

Figure 8. Block diagram of the inner and outer controllers

IV. Proposed Multi-terminal HVDC Model

A multi-terminal VSC-HVDC (MTDC) consists of three or more VSC terminals with different control objectives. A three terminal VSC-HVDC connecting an offshore wind park, a platform and an onshore grid is proposed and analyzed in this paper. The schematic diagram of the proposed MTDC is shown in Figure 9.

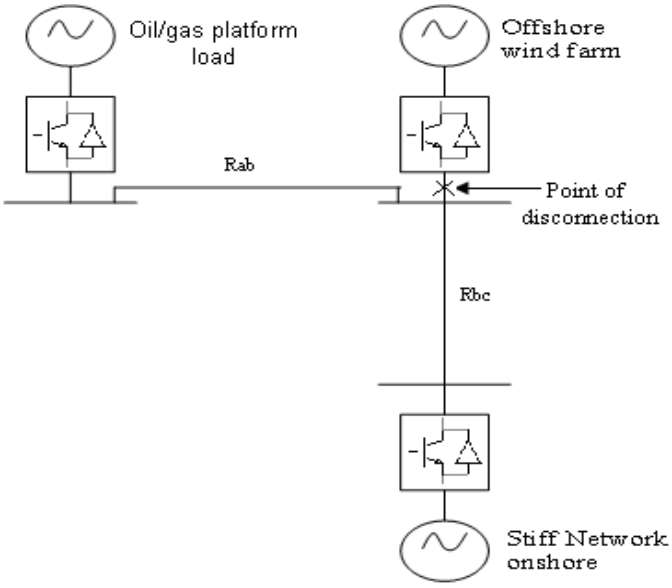

Figure 9. Proposed interconnection of platform, offshore wind farm and onshore grid

It is assumed that the offshore wind farm will supply power both to the platform and to onshore grid. During loss of the wind park terminal, the onshore grid should be able to secure power supply to the platform without a communication system between terminals. The platform is assumed to consist of passive loads. A control scheme called voltage margin method can result in the desired performance characteristics of the MTDC system [5].

According to the voltage margin method, each converter will regulate the DC voltage as long as the power flow through it is within the upper and lower limits and the reference DC voltages of the terminals are offset from one another by a certain voltage margin. This is shown in Figure 10 and Figure 11.

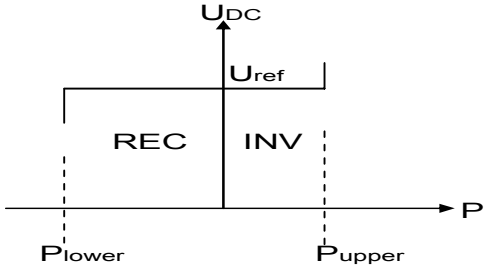

Figure 10. P, U_{DC} characteristic of a converter connected to an active system

When the upper or lower limit is passed, the terminal starts to act as a constant power terminal. The operating DC voltage will be at the point where the following relation is satisfied.

$$P_A + P_B + P_C + \cdots = 0 \tag{20}$$

Where A, B and C refer to onshore grid, offshore wind farm and oil/gas platform respectively.

This point lies in a horizontal line section of the P-U curve of one of the VSC terminals as can be seen in Figure 11. This voltage determining terminal will act as a dc slack bus and will compensate for variations in power flow.

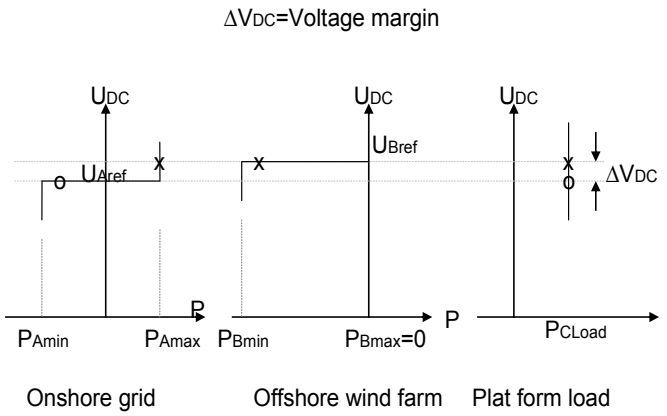

Figure 11. U-P characteristics and operating points of terminals

Negative power in the U_{DC}-P curve of Figure 10 indicates rectifier mode and positive power indicates inverter mode. The wind farm is expected to supply power up to its rated capacity and P_{Bmax} is set to zero assuming that there is no other load connection at the wind farm. Onshore grid on the other hand has an upper limit (P_{Amax}) equal to the scheduled power flow (P_{ref}) from offshore park to onshore. It should be noted that P_{ref} can be varied by an operator at onshore grid connection. The lower limit (P_{Amin}) should at least be equal to the maximum power demand of load at the platform (P_{Cmax}). This ensures that there will be uninterrupted power supply to the platform even during loss of the wind farm. Figure 11 shows that the P-U characteristic curve of the VSC that supplies power to passive network is vertical line. This is because the load depends only on the AC voltage whereas the AC voltage is kept constant independently of the DC voltage. An important feature of using voltage margin method with MTDC is that during loss of one VSC-HVDC terminal, the MTDC will maintain normal operation as long as the power transmission limits are not exceeded at each station [5]. If the terminal lost is a DC voltage regulating bus, the MTDC will

automatically find another equilibrium point and the duty of maintaining the DC voltage will be instantaneously transferred to a different terminal.

In order to get the U_{DC}-P curves shown in Figure 11, the controllers at terminals A and B will be modified as in Figure 12 [5].

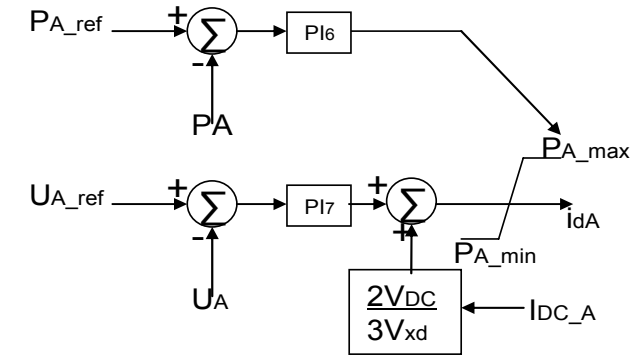

$P_{A\_min}=P_{C\_max}$ (for secured supply to platform)

A. Onshore grid

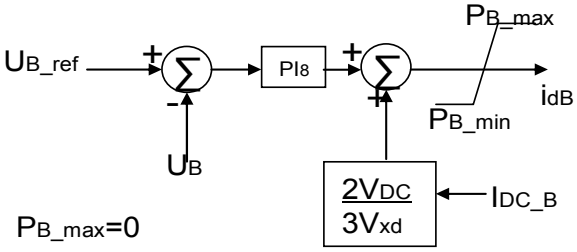

$P_{B\_max}=0$

P_{B_min}= Generating capacity of wind farm

B. Offshore wind farm

Figure 12. Outer controllers modified by voltage margin method

The DC voltage margin is given by:

$$U_{B\_ref} - U_{A\_ref} = U_{margin} = \Delta V_{DC} \quad (21)$$

The DC voltage margin should be sufficient enough to avoid interaction of the DC voltage controllers of terminal A and B during DC voltage disturbances while all the terminals are in operation.

V. Simulation Studies

To validate the idea of multi-terminal system proposed for integration of offshore wind farms and platforms into main grid, a three terminal VSC-HVDC system has been modeled and analyzed using PSCAD/EMTDC simulation software. For all converters r=0.4 Ohm, L=0.0048H and C=400uF. The switching frequency in all the three cases was set to 5 kHz. DC cables were represented by series resistances of $R_{ab}=R_{bc}$=0.01Ohm.

The following reference values were used for the terminal controllers.

Table 1. Reference value settings for controllers

Terminal	Pmax	Pmin	Uref
A. Onshore grid	40MW	-60MW	48KV
B. Offshow wind farm	0	-60MW	52KV
C. Platform load	20MW	0	24.5KVrms line to line

For both onshore grid and offshore wind farm, the parameters for the current PI controllers are: PI_1 and PI_2, $K_1=K_2$= 0.0824 $T_1=T_2$=0.0068. The DC voltage controllers in both cases are set to K_6=-2, T_3=-0.01 and the reactive power controllers are set K_4=0 T_4=-2. Active power controller at onshore grid connection has K_4=0.1 T_4=0.5. The ac voltage controller at the platform has K_5=3 T_5=0.05.

The following table summarizes the events that were run on the simulation for analysis.

Table 2. Description of simulated events

Time (sec)	Event
0	System start up
3	12MW Load connection at platform
8	Onshore grid set to draw 40MW power
12	6.5MW more load connected at platform
17	Connection to Offshore wind farm lost (at point X in Fig 8)

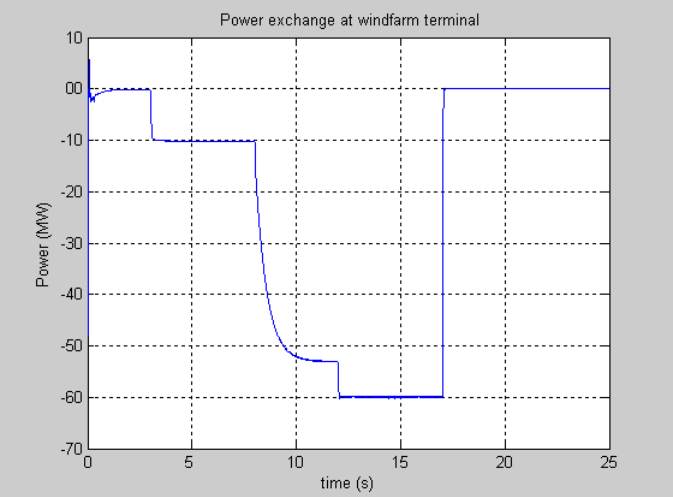

Figure 13. Power generation at the wind farm

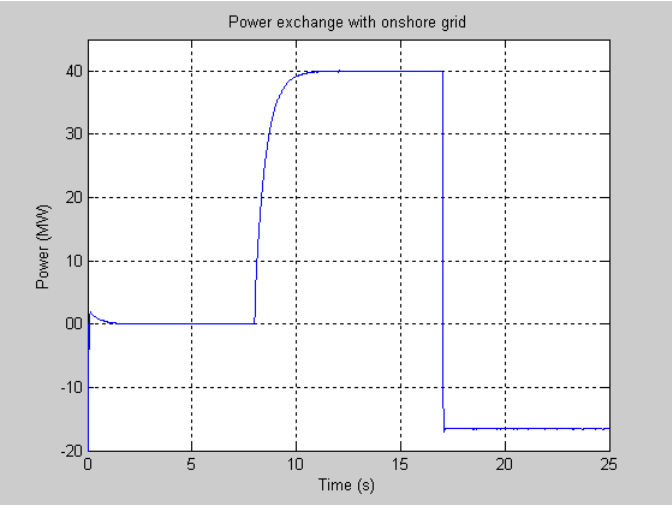

Figure 14. Power exchange with the on shore grid

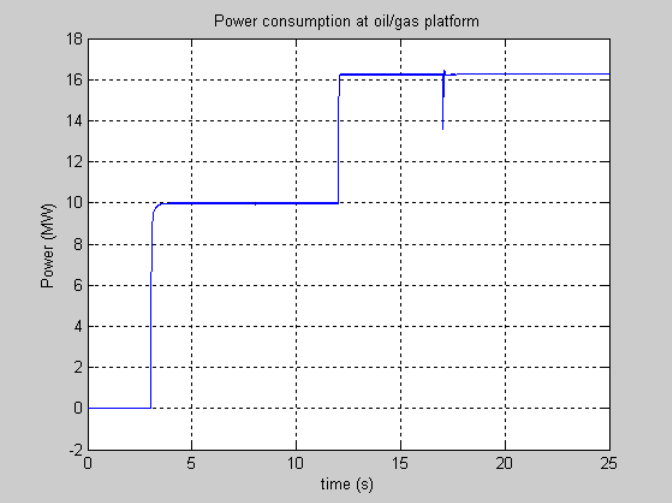

Figure 15. Power consumption at the platform

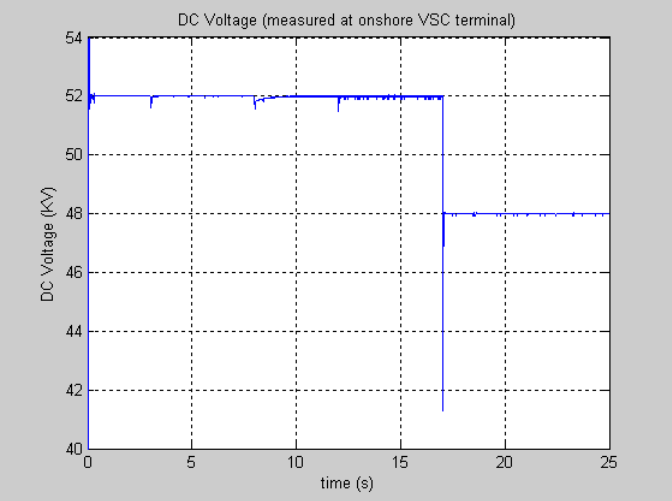

Figure 16. DC Voltage of the MTDC system

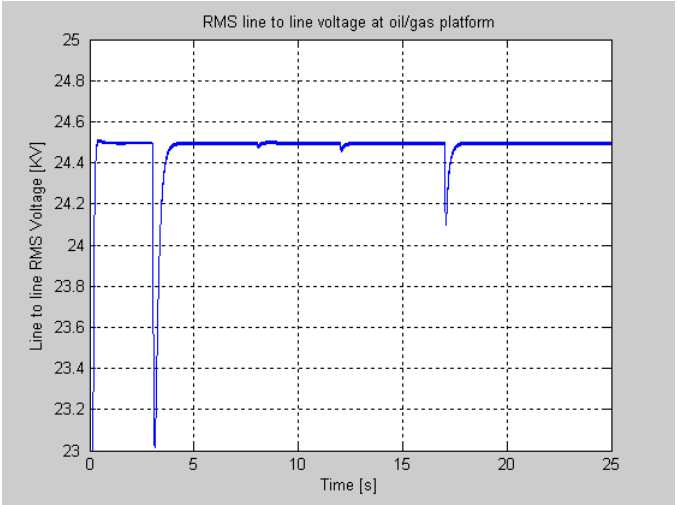

Figure 17. Line to line rms voltage at oil/gas platform load

Figure 13- Figure 17 show that the MTDC has only small steady state error and is stable under severe disturbances. The plots show that change in power reference at onshore grid (at *t*=8sec) and load switchings at platform (at *t*=3sec and *t*=12sec) have caused only minor oscillations on the DC voltage and these oscillations are effectively attenuated quickly. It is also seen that when connection to the wind farm terminal was lost, the onshore grid instantly started to supply the load demand at the platform and also maintained a new constant DC voltage level in the MTDC system. As Figure 14 shows, the power supply to the passive loads at the platform was not affected by the loss of connection to the wind farm.

CONCLUSION

In this paper a three terminal MTDC connecting offshore wind farm, oil & gas platform load and onshore grid was proposed. Equivalent circuit of VSC in d-q reference frame was established and used for developing control strategy for the multi-terminal VSC. This together with voltage margin method was used to control the MTDC system for a stable steady state and dynamic performance. Simulation results have confirmed that the proposed control results in a stable steady state and dynamic state operation and is also capable of restoring operation during loss of DC voltage regulating terminal without the need of communication between terminals.

REFERENCES

[1] GJohn Olav Gjaever Tande, "Grid Connection of Deep Sea Wind Farms – Options and Challenges", SINTEF Energy research, www.we-at-sea.org/docs/sessie 3_ tande deep sea grid iea annex 23.pdf, accessed on May 8, 2008

[2] ABB Power Technologies, "HVDC Light for Offshore Installations", www.abb.com/hvdc accessed on Feb 28, 2008

[3] Gengyin Li, Ming Yin, Ming Zhou, Chengyong Zhao, "Modeling of VSC-HVDC and Control Strategies for Supplying both Active and Passive Systems", IEEE Power Engineering Society General Meeting, pp 6, 2006.

[4] Jan Machowski, Janusz W. Bialek, Jams R. Bumby, "Power System Dynamics and Stability"; John Wiley & Sons, West Sussex pp.327, 1997

[5] Tashuhito Nakajima. Shoichi Irokawa, “A control System for HVDC Transmission by Voltage Sourced Converters”, IEEE Power Engineering Society Summer Meeting, pp. 1113-1119, 1999.
[6] Hobby Projects, “Phase Lock Loop Tutorial” www.hobbyprojects.com/block_diagrams/phase_locked_loop.html, accessed on May 14, 2008
[7] Norbert Christi, “Power Electronics at the Cable Ends”, 27-03-2006 Symposium , TU Eindhoven, Netherlands
[8] ABB Power Technologies, “Powering Valhall platform with HVDC Light®”, Brochure, www.abb.com/hvdc, accessed on May 14, 2008
[9] Bo Normark, Erik Koldby Nielsen “Advanced power electronics for cable connection of offshore wind”, Paper presented at Copenhagen Offshore Wind 2005
[10] Peter Jones, Lars Stendius, “The Challenges of Offshore Power System Construction. Troll A, Electrical Power Delivered Successfully to an Oil and Gas Platform in the North Sea”, EWEC 2006 Athens.
[11] Lars Weimers, HVDC Light, the Transmission Technology of the future, Orkuþing 2001 pp. 185-191
[12] Ned Mohan, “Advanced Electric Drives”, MNPERE, Minneapolis, pp. 3-11, 2001.
[13] Mohan, Undeland, Robbins, “Power Electronics *Converters, Applications and Design*”, John Wiley & Sons, pp. 226, 2003.